Medical Engineering & Physics xxx (2014) xxx–xxx

Contents lists available at ScienceDirect

Medical Engineering & Physics

journal homepage: www.elsevier.com/locate/medengphy

Morphological and stent design risk factors to prevent migration phenomena for a thoracic aneurysm: A numerical analysis

H.-E. Altnji*, B. Bou-Saïd[1], H. Walter-Le Berre[2]

Laboratoire de Mécanique des Contacts et des Structures, INSA de Lyon, 18-20 rue des Sciences, 69621 Villeurbanne, France

ARTICLE INFO

Article history:
Received 20 September 2013
Received in revised form 21 August 2014
Accepted 30 September 2014

Keywords:
Aortic aneurysm
Migration
Type I endoleak
Finite element
Self-expanding stent

ABSTRACT

The primary mechanically related problems of endovascular aneurysm repair are migration and type Ia endoleaks. They occur when there is no effective seal between the proximal end of the stent-graft and the vessel. In this work, we have developed several deployment simulations of parameterized stents using the finite element method (FEM) to investigate the contact stiffness of a nitinol stent in a realistic Thoracic Aortic Aneurysm (TAA). Therefore, we evaluated the following factors associated with these complications: (1) Proximal Attachment Site Length (PASL), (2) stent oversizing value ($O\%$), (3) different friction conditions of the stent/aorta contact, and (4) proximal neck angulation α.

The simulation results show that PASL > 18 mm is a crucial factor to prevent migration at a neck angle of 60°, and the smoothest contact condition with low friction coefficient ($\mu = 0.05$). The increase in $O\%$ ranging from 10% to 20% improved the fixation strength. However, $O\% \geq 25\%$ at 60° caused eccentric deformation and stent collapse. Higher coefficient of friction $\mu > 0.01$ considerably increased the migration risk when PASL = 18 mm. No migration was found in an idealized aorta model with a neck angle of 0°, PASL = 18 mm and $\mu = 0.05$. Our results suggest carefully considering the stent length and oversizing value in this neck morphology to strengthen the contact and prevent migration.

1. Introduction

Aortic aneurysm disease is characterized by a dilatation of the aorta as a result of weakness in the aorta wall. This leads to changes in wall tension with reduced tensile strength and finally rupture. Therefore, it is essential that aneurysms be repaired prior to fatal rupture. Two treatment strategies are possible: traditional surgery and endovascular aneurysm repair (EVAR) procedures. EVAR proposes a less invasive form of treatment and has undergone a dramatic technological evolution. An endovascular stent graft is a device used to seal off the aneurysm from inside the aorta providing a new pathway for the blood flow through the region of an aneurysm.

The main mid- and long-term mechanical related complications of EVAR are migration and type Ia endoleaks [1]. An endoleak is defined as the presence of blood flow outside the lumen of the endoluminal graft, but within the aneurysm sac. Type Ia endoleak occurs when there is an ineffective seal of the aneurysm sac at the proximal attachment zone of the endograft device [2,3] which allows a direct blood flow into the aneurysm sac. The flow will exert a pressure force on the aorta wall which can lead to rupture. Migration is defined as an endograft movement proximally greater than 10 mm which leads to type Ia endoleak. These complications have undergone clinical investigation and can be related to one or all of these Deployment Failure Factors (DFF): endograft undersizing [4,5], high drag forces due to severe angulation [6,7], and insufficient length of the proximal attachment site [8,9]. Most numerical research using Computational Solid Mechanics (CSM) has focused on coronary stent deployment mechanisms [10–13] or intracranial aneurysm [14]. Certain authors [15] have demonstrated the efficiency of CSM by experimental validation of the numerical results [16] of two commercial stent grafts subject to severe bending tests. More recently, investigations [17] have been conducted using CSM examining the previous complications, however, this work focused mainly on idealized vessel geometry and an unrealistic 3D geometric-connected stent behavior without investigating the mechanism of proximal stent migration. Moreover, stent collapse [18] or eccentric deformation in severe neck angulation has

* Corresponding author. Tel.: +33 4 72 43 84 52; fax: +33 4 78 89 09 80.
E-mail addresses: hussameddinaltnji86@gmail.com (H.-E. Altnji), benyebka.bou-said@insa-lyon.fr (B. Bou-Saïd), helene.walter-le-berre@insa-lyon.fr (H. Walter-Le Berre).
[1] Tel.: +33 4 72 43 84 47; fax: +33 4 78 89 09 80.
[2] Tel.: +33 4 72 43 71 88; fax: +33 4 72 43 89 13.

http://dx.doi.org/10.1016/j.medengphy.2014.09.017
1350-4533/

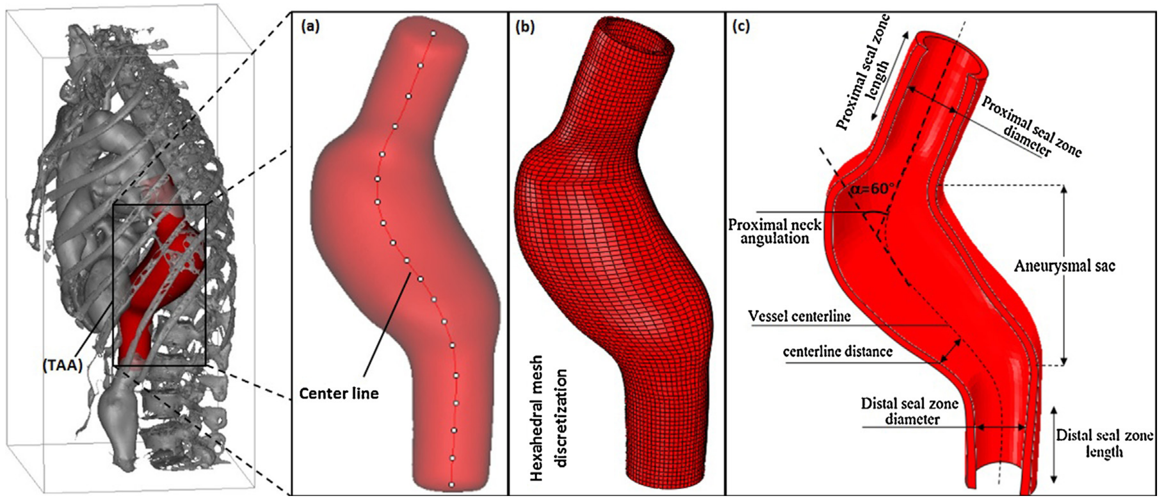

Fig. 1. (a) 3D reconstruction of aorta with centerline extraction. (b) Hexahedral mesh discretization. (c) The main definitions regarding the morphological criteria for (TAA).

not yet been examined. In another study by Prasad et al. [19] aimed at investigating the type III endoleak, stented endografts were subjected to displacement forces to investigate the contact stability at the intermodular junctions of a multi-component thoracic endograft in patient-specific TAA. However, the contact stability at proximal and distal attachment sites was not evaluated as the interaction of the aorta/stent graft at these sites was considered to be perfect.

The present paper is a follow-up to our previous paper [20] which was the premise of this project. The main advantages of this work are to find, based on a 3D FEM platform, the mechanical, morphological, and stent design factors which lead to stent migration and can cause stent collapse or poor contact between the stent and the aorta at the attachment sites. This was accomplished by evaluating the contact stiffness in the stent/aorta interaction area after stent deployment using a Coulomb frictional model in a short-term stent fixation frame. Therefore, seven parameterized stent models were used to evaluate the following DFF in a patient-specific TAA: (1) the Proximal/Distal Attachment Site Length, (2) the stent Oversizing values (O%), (3) different stent/aorta contact friction conditions, and (4) the proximal neck angulation (α).

2. Materials and methods

2.1. Patient specific TAA and stent models

The FEM patient-specific TAA model was the same as for the previous work [20], starting from the planar slices obtained from the clinical CT scans in plane resolution. The reconstruction interval equals to the slice thickness of 0.73 mm. The pre-stenting vessel centerline was calculated to guide stent positioning. The meshing of the finite elements was developed using C3D8R element type as shown in Fig. 1.

Although the anisotropy of the wall properties has been well recognized [21–23], the blood vessel in our case can be considered as isotropic as the degree of anisotropy is small [24,25]. In the Abaqus/Explicit software package used, we must provide sufficient compressibility for the code to work. It was defined as $K_0/\mu_0 = 20$ where K_0 is the initial bulk modulus and μ_0 the initial shear modulus. The material was considered as isotropic hyperplastic, and nearly incompressible. The decoupled representation of the strain-energy function $\Psi = \Psi(C)$ is given by the function,

$$\Psi(C) = \Psi_{vol}(J) + \Psi_{iso}(\bar{C}), \tag{1}$$

where $\Psi_{vol}(J)$ and $\Psi_{iso}(\bar{C})$ describe the so-called volumetric elastic response, and the isochoric elastic response of the material, respectively [26]. The generalized Mooney–Rivlin hyperelastic constitutive model was used. The decoupled polynomial representation of the strain energy function is given by,

$$\Psi = \sum_{i+j=1}^{N} C_{ij}(\bar{I}_1 - 3)^i(\bar{I}_2 - 3)^j + \sum_{i=1}^{N} \frac{1}{D_i}(J - 1)^{2i}, \tag{2}$$

where N, C_{ij} and D_i are temperature-dependent material parameters. The strain invariants are denoted $\bar{I}_1$ and $\bar{I}_2$. The symbol J is the volume ratio or the elastic volume strain, while D_i describes the compressibility of the material. The hyperelastic constants were determined from the experimental tests [27]. Only radial displacements of the nodes located on the upper and bottom surfaces were allowed. We assumed no internal and external pressure on the aneurysm. The effects of residual stresses [1,23] were also neglected given the fact that blood vessels can be in a nearly stress-free state when they are free from external loads [24]. The nominal uniform thickness was considered to be 3 mm [28].

The stent geometric models were generated by means of a specially developed parameterization algorithm, using global variables (all in mm) $ST_{OD} = 17$, $S_{TH} = 0.6$, $S_L = 21$, $B_W = 0.7$, $S_{VW} = 0.8$, $G = 4.6$, $G_{SC} = 23.5$ mm illustrated in Fig. 2a. Other variables (Y_{strut}, S_W, R_1, R_2, S_{LS}) were linked to previous ones by the equations given in Fig. 2a, where R_1 and R_2 are the inner and outer radius of strut vertex, respectively. We denote Y_{strut} as a circumferential distance of a single strut at the given diameter, and $N_{struts} = 10$ is the number of struts around the circumference of the stent. The stent was modeled starting from the master sketch with six strut columns along the stent. The 3D parametric stent model was then created with suitable operations in the CATIA V5R20 software. All stent models were carefully discretized with the C3D8R element type using hourglass control [29]. In order to produce accurate representation of the actual stent geometry, the CAD stent model was driven by a rigid cylindrical surface, accomplishing the needed oversizing value relative to the outer diameter of the aorta, as shown in Fig. 2b. In the shape setting simulation, nitinol was considered to be an elastoplastic material [30]. Then, the expanded stent model was added back into the assembly model in a strain-free manner. After mesh convergence analysis (see Appendix), we applied three elements through the thickness, and four elements across the width with a reasonably refined mesh of the strut (Fig. 2b).

In the deployment procedure, superelastic behavior of the nitinol was assigned to the stent. The numerical implementation of